Intra- and Intermolecular Cooperativity in the Catalytic Activity of Phosphodiester Cleavage by Self-Assembled Systems Based on Guanidinylated Calix[4]arenes

Chemistry - A European Journal

Intra- and Intermolecular Cooperativity in the Catalytic Activity of Phosphodiester Cleavageby Self-Assembled Systems Based on Guanidinylated Calix[4]arenes.

--Manuscript Draft--

Manuscript Number:	
Article Type:	Research Article
Corresponding Author:	Riccardo Salvio, Ph.D University of Rome Tor Vergata: Universita degli Studi di Roma Tor Vergata Roma, ITALY
Corresponding Author E-Mail:	riccardo.salvio@uniroma2.it
Order of Authors (with Contributor Roles):	Daniele Lisi
	Carlo Alberto Vezzoni
	Alessandro Casnati, Prof.
	Francesco Sansone, Prof.
	Riccardo Salvio, Prof.
Keywords:	Supramolecular catalysis; artificial phosphodiesterases; enzyme mimics; self-assembling; calixarenes.
Manuscript Classifications:	Aggregation; Calixarenes; Homogeneous catalysis; Self-assembly; Supramolecular chemistry
Suggested Reviewers:	Bim Graham Monash University bim.graham@monash.edu
	Pablo Ballester ICIQ: Institut Catala d'Investigacio Quimica pballester@iciq.es
	Anatoly Yatsimirsky Universidad Nacional Autónoma de México Facultad de Química: Universidad Nacional Autonoma de Mexico Facultad de Quimica iatsimirski46@comunidad.unam.mx
	Tuomas Lönnberg University of Turku tuanlo@utu.fi
	R. Stan Brown Queen's University stan.brown@chem.queensu.ca
	Jack Chen University of Siena: Universita degli Studi di Siena jack.chen@unisi.it
	Ivan Jabin Université Libre de Bruxelles: Universite Libre de Bruxelles ivan.jabin@ulb.be
Opposed Reviewers:	
Abstract:	Calix[4]arene scaffold, blocked in the cone conformation through alkylation with long alkyl chains, and decorated at the upper rim with four guanidine or arginine units, effectively catalyzes the cleavage of the phosphodiester bond of DNA and RNA model compounds in water. An exhaustive kinetic investigation unequivocally points to the existence of spontaneous aggregation phenomena, driven by hydrophobic interactions, occurring at different critical concentrations that depend on the identity of the compound. A pronounced superiority of the assembled structures compared with the monomers in solution was observed. Moreover, the catalytically active units, clustered

	on the macrocyclic tetrafunctional scaffold, were proved to efficiently cooperate in the catalytic mechanism and result in improved reaction rates compared to those of the monofunctional model compounds. The kinetic analysis is also integrated and corroborated with further experiments based on fluorescence spectroscopy and light scattering. The advantage of the supramolecular assemblies based on tetrafunctional calixarenes leads to believe that the active units can cooperate not only intramolecularly but also intermolecularly. The molecules in the aggregates can probably mold, flex and rearrange but, at the same time, keep an ordered structure that favor phosphodiester bond cleavage. This dynamic preorganization can allow the catalytic units to reach a better fitting with the substrates and perform a superior catalytic activity.
Author Comments:	Dear Editor, Respected colleagues acting as referees, accompanying this letter please find a manuscript entitled “Intra and Intermolecular Cooperativity in the Catalytic Activity of Phosphodiester Cleavage by Self-Assembled Systems Based on Guanidinylated Calix[4]arenes.”, which me and my coworkers, Prof. Sansone and Prof. Casnati, wish to submit for publication as an Article in Chemistry - A European Journal. In this paper we report about the study of the phosphodiesterase activity of calix[4]arenes blocked in the cone conformation by alkylation with long hydrophobic alkyl chains and decorated at the upper rim with four arginine or guanidinium units. The use of the calix[4]arene scaffold is motivated by the extreme versatility and efficiency of this platform that turned out to be an excellent compromise between preorganization and flexibility. As argued in the manuscript, this is an essential requisite to obtain high catalytic activity. We carried out an exhaustive kinetic investigation of the catalytic activity of the calixarenes and their corresponding monofunctional analogs in the cleavage of RNA and DNA model compounds. These data are also corroborated and integrated with further experiments based on fluorescence spectroscopy and light scattering. The data collected in this study unequivocally point to the existence of aggregation phenomena, driven by hydrophobic interactions, occurring at different critical concentrations, depending on the identity of the compounds. A marked superiority of the catalytic activity of the aggregates, in comparison with the monomers in solution, was observed. The efficiency of the catalysts is discussed in terms of cooperativity, a parameter which provides a quantitative indication of the preorganization of the catalytic system and a measure of the synergism of the active functions. The issue of inter and intramolecular cooperativity and the concept of dynamic preorganization is discussed in the manuscript. We believe that the data reported in the present manuscript add considerably to the present knowledge in the area of catalysis by design, enzyme mimics, chemistry of calixarene derivatives, and study of reaction mechanisms. In addition, the present study can also provide interesting data to researchers committed in the field of aggregates, colloids, and liposomes. Consequently, we hope it will attract the interest of a vast readership. Moreover, we believe that the present work is fully appropriated for the audience of Chemistry – A European Journal because it perfectly fits the scope and specification of the journal, and also because previous investigations on similar research lines have been reported, by our group (e.g. Chem. Eur. J. 2015, 21, 5856) and by others, on this journal. In conclusion, for the reasons illustrated above, we kindly ask you to consider the present paper for publication in Chemistry – A European Journal as an article. Looking forward to hearing from you, I remain Best Regards Riccardo Salvio, PhD on behalf of all the authors
Section/Category:	
Additional Information:	
Question	**Response**
Do you agree to comply with the legal and	Yes

ethical responsibilities outlined in the journal's Notice to Authors?	
Has a previous version of this manuscript been submitted to this journal?	No
Is this manuscript, or part of it, currently under consideration elsewhere?	No
Is this manuscript, or part of it, published, posted, or in press? This includes content posted on preprint servers (preprint guidelines) or published as part of a thesis.	No
Please provide us with information about the history of your manuscript, including previous submissions, transfers, or prior versions:	first submission
Does the research described in this manuscript include animal experiments?	No
Does the research described in this manuscript include human research participants (including for experiments with sensors or wearable technologies) or tissue samples from human subjects (including blood or sweat)?	No
Do you or any of your co-authors have a conflict of interest to declare?	No
This journal supports data sharing and has adopted an Expects Data Sharing policy: - You are encouraged to make your data available, for instance in a public repository. - Your article must include a Data Availability Statement; please select a template from the options below or provide a custom Statement. - When data is openly available, please provide the name and URL/DOI of the repository and cite the data in the references section of your manuscript.	Data available in article supplementary material

Is your data available?	
Please confirm the selected template for your Data Availability Statement below, which will be published as part of your article if it is accepted for publication. as follow-up to "This journal supports data sharing and has adopted an Expects Data Sharing policy: - You are encouraged to make your data available, for instance in a public repository. - Your article must include a Data Availability Statement; please select a template from the options below or provide a custom Statement. - When data is openly available, please provide the name and URL/DOI of the repository and cite the data in the references section of your manuscript. **Is your data available?"**	The data that support the findings of this study are available in the supplementary material of this article.

Intra- and Intermolecular Cooperativity in the Catalytic Activity of Phosphodiester Cleavage by Self-Assembled Systems Based on Guanidinylated Calix[4]arenes.

Daniele Lisi,[a‡] Carlo Alberto Vezzoni,[b‡] Alessandro Casnati,[b] Francesco Sansone,[b*] Riccardo Salvio,[a,c*]

[a] Dipartimento di Scienze e Tecnologie Chimiche, Università "Tor Vergata", Via della Ricerca Scientifica, 1, I-00133 Roma, Italy.

[b] Dipartimento di Scienze Chimiche, della Vita e della Sostenibilità Ambientale, Università degli Studi di Parma, Viale delle Scienze, 17/A, 43124 Parma, Italy

[c] ISB - CNR Sezione Meccanismi di Reazione, Università La Sapienza, 00185 Roma, Italy.

* To whom the correspondence should be addresses: francesco.sansone@unipr.it, riccardo.salvio@uniroma2.it

‡ The authors equally contributed to the present work.

Abstract

Calix[4]arene scaffold, blocked in the cone conformation through alkylation with long alkyl chains, and decorated at the upper rim with four guanidine or arginine units, effectively catalyzes the cleavage of the phosphodiester bond of DNA and RNA model compounds in water. An exhaustive kinetic investigation unequivocally points to the existence of spontaneous aggregation phenomena, driven by hydrophobic interactions, occurring at different critical concentrations that depend on the identity of the compound. A pronounced superiority of the assembled structures compared with the monomers in solution was observed. Moreover, the catalytically active units, clustered on the macrocyclic tetrafunctional scaffold, were proved to efficiently cooperate in the catalytic mechanism and result in improved reaction rates compared to those of the monofunctional model compounds. The kinetic analysis is also integrated and corroborated with further experiments based on fluorescence spectroscopy and light scattering.

The advantage of the supramolecular assemblies based on tetrafunctional calixarenes leads to believe that the active units can cooperate not only intramolecularly but also intermolecularly. The molecules in the aggregates can probably mold, flex and rearrange but, at the same time, keep an ordered

structure that favor phosphodiester bond cleavage. This dynamic preorganization can allow the catalytic units to reach a better fitting with the substrates and perform a superior catalytic activity.

Introduction

The interaction between different functional groups and the substrate is at the base of the operation of enzymes and a large number of artificial catalysts.[1] The simultaneous action of the functional groups decreases the activation energy of the catalyzed reaction of a much greater extent than that expected from the interactions with the active units singularly. This effect is commonly referred to as cooperativity.[2-4] A number of different strategies have been developed in order to keep the functional groups directly involved in the catalytic process at the right distance and at the proper orientation. These strategies include the use of conventional molecular scaffolds,[5-7] dendrimers,[8] polymers[9-10] and nanoparticles.[6, 11-13] In these systems the active functional groups are kept close to each other, through covalent bonds, in order to guarantee the best cooperativity. However, it is necessary to avoid an exceedingly rigid structure as significant catalytic activity and cooperativity always arises from a good compromise between preorganization and flexibility.[14-16]

Given the importance of phosphodiester bonds in living organisms and their reluctance to undergo spontaneous hydrolysis,[17-18] a number of researchers developed enzyme mimics able to efficiently cleave DNA, RNA and their model compounds.[1, 15, 19-29] In most of these artificial phosphodiesterases metal cations are employed as active functions, with the role of Lewis acid activators, binding sites, nucleophile carriers and promoters of leaving group departure.[26, 30-37]

In the last decade, we dedicated our attention to the study of the cooperative action of guanidinium units by themselves,[22, 24, 38-39] or in conjunction with other active units,[25, 40] in the cleavage of phosphodiester bonds in DNA and RNA model compounds. In these studies, diverse approaches were used to place the functional groups at close distance, ranging from the simple diphenylmethane scaffolds[38] to silica nanoparticles-grafted polymer brushes.[41] In this respect, calixarenes provide an excellent option to realize multifunctional catalysts as they can be repeatedly functionalized either at the upper rim and at the lower rim with remarkable versatility.[16, 42]

In this study we present a systematic investigation about the multifunctional guanidinium-decorated calix[4]arenes **3**-**5**, functionalized with guanidine and arginine units, able to self-assemble in water solution into more complex structures through hydrophobic interactions. Interestingly, these compounds are catalytically active both as free monomers in solution and organized in polymolecular aggregates. The use of self-assembled aggregates, whose formation is driven by weak interactions,

may provide a number of advantages versus catalysts exclusively based on active units covalently linked to a scaffold. Among these potential advantages there is the possibility to build, in a synthetically more accessible manner, a highly multifunctional system able to better adapt to substrates and feature dynamic preorganization.

The phosphodiesterase activity of the corresponding monofunctional model compounds **1** and **2** was also investigated for comparison. The issue of inter- and intramolecular cooperativity will be discussed.

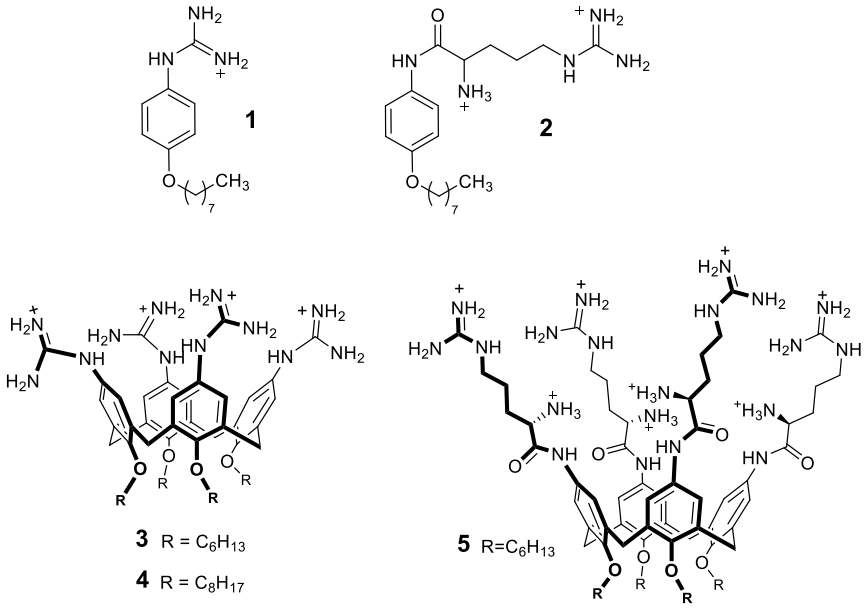

2. Results and Discussion

2.1 Synthesis of the catalysts

The syntheses of monofunctional guanidinium and arginine derivatives **1** and **2** were carried out according to Scheme 1. *p*-Nitrophenol was alkylated with 1-bromooctane and the nitro group reduced in the presence of hydrazine and Pd/C as catalyst. The guanidinylation reaction on aminoderivative **6** was carried out using *N*,*N*′-bis-(*t*-butoxycarbonyl)-*N*″-triflyl-guanidine affording compound **7**. The protecting group removal was achieved with an aqueous solution of TFA, and a counter ion exchange with an excess of hydrochloric acid (Scheme 1, *e*) was carried out. For the synthesis of the arginine derivative **2**, the aniline **6** was reacted with the corresponding protected amino acid Boc-L-Arg-PbfOH in the presence of *N*,*N*'-dicyclohexylcarbodiimmide as coupling agent. To avoid an acyl transfer forming the unreactive *N*-acylurea as an isomerization side reaction,[43] an equivalent of

hydroxybenzotriazole was added to the reaction mixture. This nucleophile reacts faster than the competing acyl transfer and generates an intermediate still active enough to couple with the aniline affording compound **8**. Furthermore, this reagent prevents the racemization occurring through formation of the oxazolone.[44] The simultaneous removal of both protecting groups was carried out in a TFA/MeOH/triisopropyl silane mixture.

The calixarenes **3**-**5** were synthesized according to previously reported procedures similar to those of the monofunctional model.[45-46]

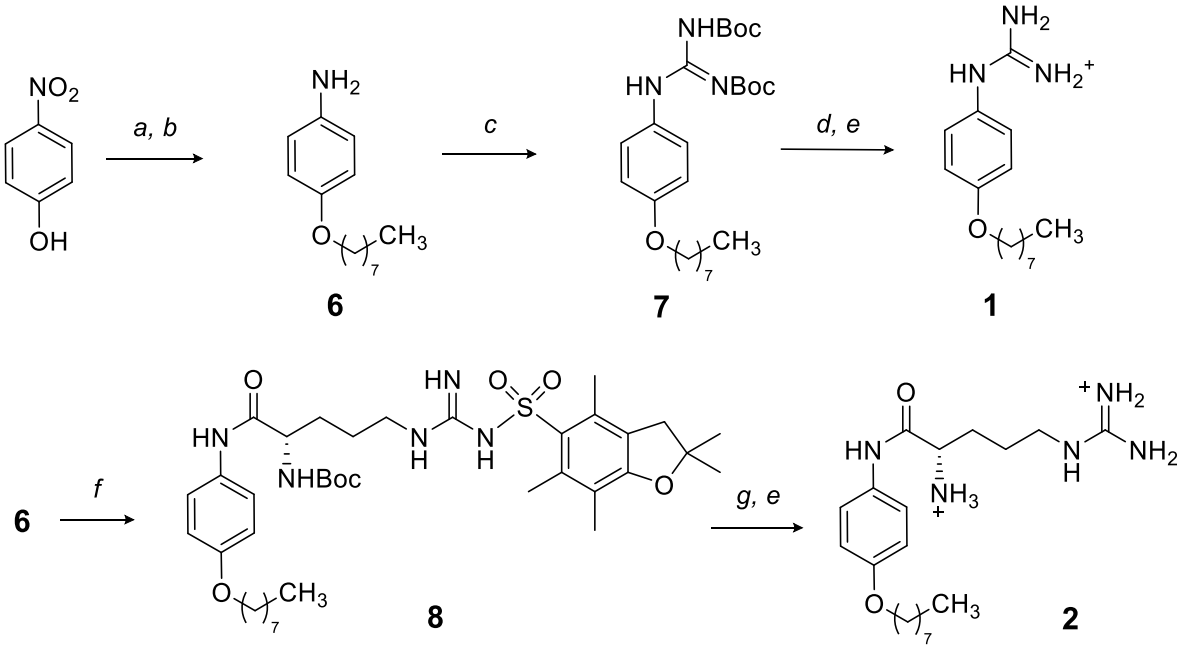

Scheme 1 Synthesis of guanidinium derivatives **1** and **2**. Reagents and conditions: (*a*) 1-bromoctane, NaH, DMF; (*b*) $N_2H_4 \cdot H_2O$, Pd/C, EtOH; (*c*) *N*,*N*′-Bis-(*t*-butoxycarbonyl)-*N*″-triflyl-guanidine, DCM; (*d*) TFA, H_2O; (*e*) HCl, EtOH. (*f*) Boc-L-Arg-PbfOH, hydroxybenzotriazole, DCC, DMF; (*g*) TFA, triisopropylsilane, MeOH.

2.2 Catalytic Measurements

A first set of kinetic measurements was carried out in the catalyzed cleavage of 2-hydroxypropyl *p*-nitrophenyl phosphate (eqn. 1) and bis-(*p*-nitrophenyl) phosphate (eqn. 2), RNA and DNA model compounds respectively. The measurements were carried out in water solution in the presence of 0.5 mM concentration of compounds **1**-**5**. According to our previous observation, the existence of a guanidine-guanidinium catalytic dyad is a requisite to observe a relevant catalytic effect.[38, 47] For this reason the pH value might be important for the catalytic performances. In addition, an elevated pH value increases the spontaneous reactivity of the substrate. Driven by previously reported data,[47] the

acidity of the solutions was buffered at pH 9.0 with *N*-cyclohexyl-2-aminoethanesulfonic acid (CHES).

Pseudo-first-order rate constants for the cleavage of 2-hydroxypropyl *p*-nitrophenyl phosphate (HPNP) and bis-(*p*-nitrophenyl) phosphate (BPNP) were calculated as $k_{obs} = v_0/[substrate]$, where v_0 is the initial rate of *p*-nitrophenol release determined via UV-Vis spectrophotometry. These values are listed in Table 1. In the same table are reported the acceleration over the spontaneous cleavage at the same pH (k_{obs}/k_{bg}) and a value k_{rel}, defined as the ratio between k_{obs} for the catalyst and the corresponding monofunctional model compound (see note c, Table 1).

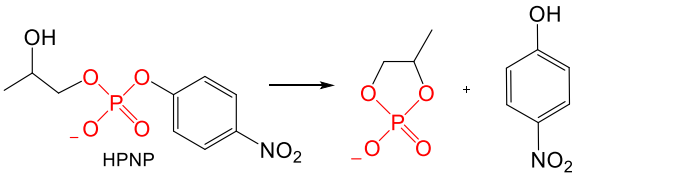

(1)

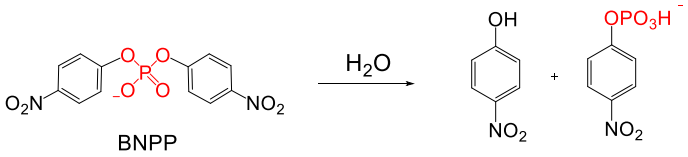

(2)

Table 1. Cleavage of HPNP and BNPP in the presence of additives 1-5[a]

		HPNP			BNPP		
entry	additive	k_{obs} (s^{-1}) [b]	k_{rel} [c]	k_{obs} / k_{bg} [d]	k_{obs} (s^{-1}) [b]	k_{rel} [c]	k_{obs} / k_{bg} [d]
1	-	1.1×10^{-6}	-	1.0	4.2×10^{-9}	-	1.0
2	**1**	2.7×10^{-6}	1	2.4	5.9×10^{-8}	1	14
3	**2**	5.2×10^{-6}	1	4.7	1.0×10^{-7}	1	24
4	**3**	5.0×10^{-5}	19	45	1.8×10^{-6}	30	430
5	**4**	4.8×10^{-5}	18	43	9.7×10^{-7}	16	230
6	**5**	1.8×10^{-4}	35	160	2.4×10^{-6}	24	570

[a] Conditions: 10 mM *N*-cyclohexyl-2-aminoethanesulfonic acid in water; 0.50 mM HPNP; 0.50 mM catalyst, 10 mM Me_4NClO_4, T = 25.0 °C, 50.0 °C for HPNP and BNPP respectively; [b] k_{obs} calculated with the initial rate methods from the following expression: $v_o/[substrate]$; error limits of k_{obs} values on the order of ±10%. [c] k_{rel} calculated as k_{obs}(catalyst)/k_{obs}(corresponding monofuntional model). [d] The background rate constant (k_{bg}, s^{-1}) for spontaneous cleavage of the substrate was measured at the same pH in the presence of a higher substrate concentration, *i.e.* 1.5 mM.

All the investigated compounds turned out to be active in the hydrolysis of both substrates. For the first time it was possible to point out that also arginine moieties act as catalytic units even though the distance of the guanidinium ions from the each other is consistently increased compared to guanidinocalixarenes **3** and **4** and the mobility of the chains is increased.

The highest accelerations were observed in the case of BNPP, *i.e.* up to 570-fold in the presence of arginine derivative **5**. This substrate exhibits a much lower spontaneous reactivity ascribable to the lack of an intramolecular nucleophilic hydroxyl, and hence is remarkably more sensitive to the presence of the catalysts. The tetrafunctional calixarenes **3**-**5** show a remarkable superiority if compared with their monofunctional model **1**-**2**, with k_{rel} values in the range 18-35. These values largely exceed the statistical factor, *i.e.* 4, due to the presence of four active units on the same molecule for catalysts **3**-**5**. This is an indication of a possible cooperativity between the guanidinium units in the calixarene molecular scaffold.

Since an in-debt kinetic analysis cannot be separated from the dependence of the catalytic performance on the concentrations, a second set of kinetic measuremets was carried out changing the catalyst concentrations in a submillimolar range for guanidinium derivatives **1**-**5**. For all the investigated compounds, a linear trend of k_{obs} versus the concentration was observed at high dilution (Figure 1). It is relevant to note that, at low concentration, the spontaneous cleavage of the substrate is not negligible compared to the catalyzed reaction, as the intercept of the line interpolating the data points is different from zero and this is in agreement with the uncatalyzed k_{obs} measured in the absence of any catalyst. At higher concentrations, different for all the investigated catalysts, a relevant discontinuity was observed with a marked increase of the rate constants. Both the regions show a linear dependence on the additive concentrations but with two different slopes (see Figure 1 and Supporting Information p. S8-10).

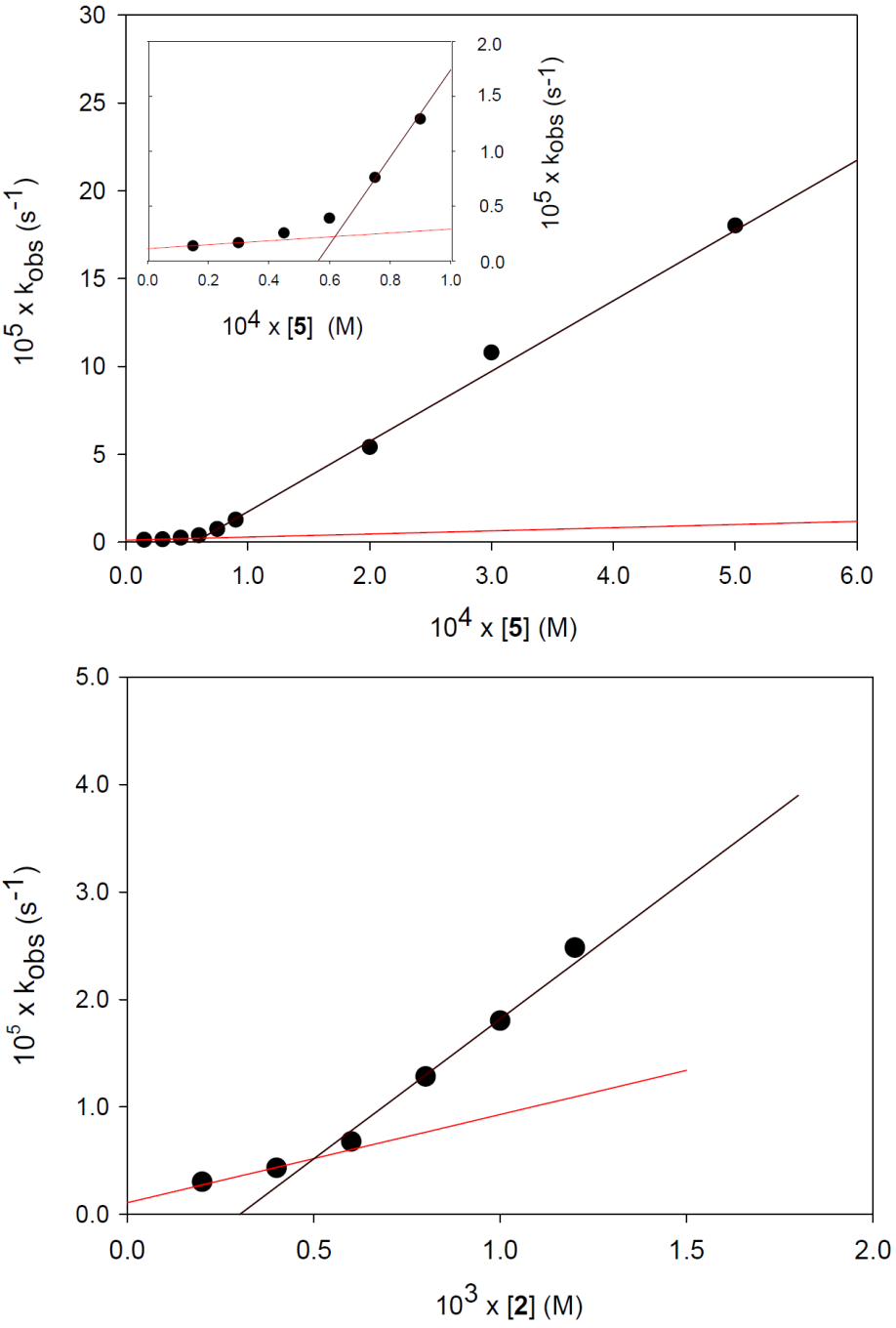

Figure 1 Plot of the observed rate constant for the HPNP transesterification catalyzed by **5** in water buffered at pH 9.0 versus the catalyst concentration and corresponding zoomed-in inset in the concentration range 0-0.1 mM (top). Transesterification of HPNP catalyzed by the monofunctional model compound **2** in the same conditions (bottom).

This experimental evidence strongly points to the existence of a spontaneous assembly at the concentration at which the two straight lines intersect, hereafter referred to as Critical Aggregation Concentration (CAC). The existence of the aggregates is also confirmed by monodimensional

^{1}H NMR and DOSY experiments that show the existence of both the monomer and the aggregate in slow exchange at the NMR timescale (see Supporting Information p. S20 and ref. [46]).

The plots of the specific rate cleavage versus the catalyst concentration do not show any saturation profile, suggesting the operation of catalysts **1**-**5** in subsaturation conditions at this concentration range (Table 1 note *a*), *i.e.* a binding constant between the substrate and the catalyst (monomer or aggregate) lower than 100 M^{-1}. For the mechanism reported in eq (3), the observed rate constant is given by eq (4). If the catalytic system operates in subsaturating conditions, the term $K[C] << 1$, and consequently eq (4) reduces to eq (5), where k_2 is a second order rate constant defined as $k_2 = k_{cat}K$. If the contribution of the monomer, the aggregate, and the spontaneous cleavage are considered, the observed rate constant is given by eq (6), where $[C]_T^{mon}$ and $[C]_T^{aggr}$ are the catalyst concentrations of the monomer in solution and in the aggregate, respectively.

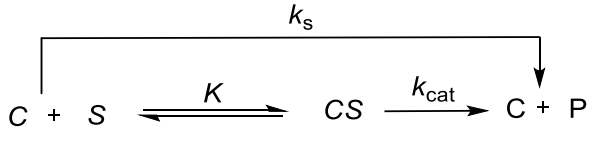

(3)

$$k_{obs} = \frac{k_{cat}K[C]+k_s}{K[C]+1} \quad (4)$$

$$k_{obs} = k_2[C]_T + k_s \quad (5)$$

$$k_{obs} = k_2^{mon}[C]_T^{mon} + k_2^{aggr}[C]_T^{aggr} + k_S \quad (6)$$

Least-square fitting procedures of the two linear regions were carried out to determine the second order rate constant k_2 calculated as the slopes of the two straight lines showed in Figure 1. The k_2 values for the monomers (k_2^{mon}) and for the aggregates (k_2^{aggr}) determined by the linear fitting below and over the concentration are reported in Table 2 for the five investigated catalysts, together with the corresponding CAC.

Table 2. Second order rate constants k_2 and Critical Aggregation Concentrations [a]

entry	additive	CAC (mM) [b]	k_2^{aggr} ($M^{-1}s^{-1}$) [c]	k_2^{mon} ($M^{-1}s^{-1}$) [d]	k_2^{aggr} / k_2^{mon}
1	**1**	1.20	4.3×10^{-2}	3.8×10^{-3}	11
2	**2**	0.68	2.6×10^{-2}	8.2×10^{-3}	3.2
3	**3**	0.095	1.2×10^{-1}	1.2×10^{-2}	10
4	**4**	0.045	1.0×10^{-1}	6.4×10^{-3}	16
5	**5**	0.062	4.0×10^{-1}	1.8×10^{-2}	22

[a] data obtained from the elaboration of data reported in Figure 1 and in Figures at p. S9-S10, Supporting Information; [b] determined from the intersection of the two straight lines, e.g. Figure 1. [c] calculated by a linear least-square fitting procedure with the points over the CAC; [d] calculated by a linear least-square fitting procedure with the data points below the CAC.

The CAC for the monofunctional derivatives **1** and **2** is around 1 mM (Table 2, entries 1 and 2). On the other hand, calixarenes **3-5** aggregate at significantly lower concentrations, CACs ≤ 0.1 mM, with the lowest value observed for calixarene **4**, provided with the longest alkyl chains at the lower rim (C_8H_{18}). Interestingly, the k_2^{aggr} / k_2^{mon} ratio provides a quantitative comparison of intramolecular and intermolecular (intra-aggregates) cooperativity. In the case of monofunctional models, no intramolecular cooperativity can be exerted as the cooperation can occur only in the aggregate. The arginine derivative **2** shows a modest synergic action in the assembly, however catalyst **1** shows an advantage of 11-fold compared to the monomer.

For the tetrafunctional calix[4]arene structures, the performances in the catalytic aggregates definitely overcome those of the unaggregated monomers in solutions, with the best advantage observed for the arginine derivative **5.**

On the basis of these data, a noteworthy superiority of the assemblies is evident in all the cases. This phenomenon might suggest that the catalytically active units can perform a better cooperativity in the substrate activation due to the existence of intermolecular cooperativity and dynamic preorganization. In other words, the catalytic system in the self-assembled aggregate could be able to rearrange, mold and flex in response to the substrate geometrical and electronic requirements also allowing catalytic groups of different monomers to cooperate. All these effects seem to be responsible to better fulfill the stabilization of the reaction transition state in the aggregates compared with the unaggregated monomers.

2.3 Fluorescence and DLS measurements

In order to gain further insights about the aggregates tested in the kinetic measurements, fluorescence measurements in the presence of pyrene were carried out. This compound features an emission spectrum that is significantly affected by the polarity of the environment, due to a different non-planar structure of the excited state compared to the ground state. In addition, it has the tendency, as an aromatic hydrocarbon, to accumulate in hydrophobic environments. Because of these properties, it has been used as a probe for microheterogeneous systems such as polymers, proteins, micelles, and membranes[48-49]

The ratio of the intensities of band I (372 nm) and band III (382 nm) in the emission spectrum is sensitive to the polarity/hydrophobicity of the environment.[50] A 2 μM solution of pyrene has been prepared in the same reaction medium (H_2O, pH 9.0 CHES, 10 mM Me_4NClO_4) and titrated with calixarene **3**. The high dilution of the fluorescent probe avoids the formation of excimers that can significantly affect the emission spectra. In the plot in Figure 2 is reported the ratio of the intensities of the band I and III (I_1/I_3) versus the logarithm of the surfactant concentration. In the early stage of the titration, the I_1/I_3 parameter is around the value 1.8. Afterwards, upon further increase of the calixarene concentration, the parameter sharply drops down. Most likely, this effect can be attributed to the inclusion of pyrene in the forming aggregate, consequently the concentration at which the slope change occurs can be regarded the critical aggregation concentration. The value of this parameter estimated with this method is in the range of 30-65 μM. This value is in fair good agreement with the CAC obtained from the kinetic measurements, *i.e.* 95 μM (Table 2, entry 3).

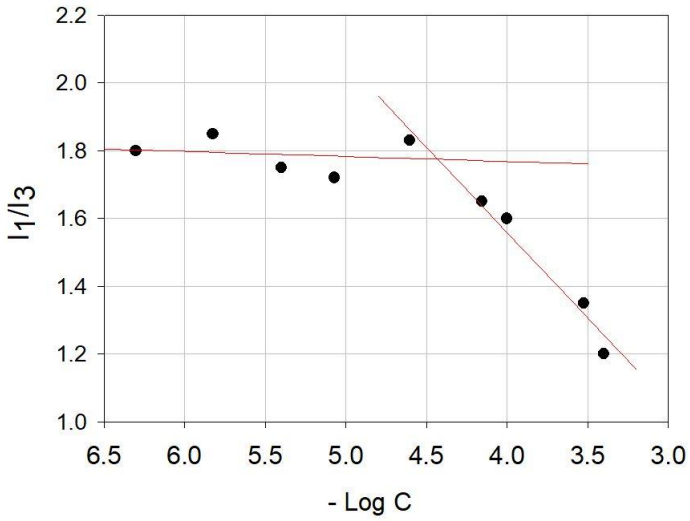

Figure 2 Spectrofluorometric titration of a 2 μM pyrene water solution (pH=9, I=10 mM) with calix[4]arene **3**. I_1/I_3 versus the logarithm surfactant concentration. The red lines are obtained by the best-fitting of the experimental data in the two regions. The CAC can be estimated from the intercept of the straight lines.

The critical packing parameter (CPP) is often taken in consideration in the literature to rationalize and predict some aspects of the molecular self-assembly in solution.[51-54] This parameter is defined as v_o/al_o, where v_o and l_o are the volume and the length of the surfactant tail, respectively, and a is the headgroup area. A Molecular Dynamic (MD) simulation carried out in a solvent box was employed to evaluate the average values of v_o, l_o and a. The CPP values calculated from the obtained parameters are reported in Table 3, together with the standard deviations. For compounds **1** – **5**, they are in the range 0.51 – 0.84. For pronounced cone-shaped surfactants the CPP values is closer to 0, on the other hand, for molecule more similar in shape to a truncated cone or a cylinder, the CPP approaches 1. According to a widespread criterion present in the literature, CPP values between 0.5 and 0.8 are compatible with rod-like micelles or a bilayered structure.[51-52]

Table 3 Critical Packing Parameter

species	CPP [a]
1	0.58 ± 0.04
2	0.51 ± 0.04
3	0.83 ± 0.05
4	0.84 ± 0.05
5	0.55 ± 0.04

[a] calculated as v_o/al_o. The geometric parameters were determined through a MD simulation. The reported error limit is the standard deviation σ.

Dynamic light scattering (DLS) is a technique able to determine the size distribution profile of small particles/aggregates in solution.[55] An analysis of a 0.25-0.5 mM water solution of calixarene **3**, at pH 9.0 and with ionic strength buffered with NMe_4NClO_4, as in the kinetic experiments. The measurements indicate the most relevant size distribution of the aggregates centered at 17 nm (see Section S6 in Supporting Information for details). The average particle size appears to be stable in a

time interval of a few hours, the timescale of the kinetic experiments, whereas particles of higher dimensions, *i.e.* 180 nm, were detected after 60 hours (see p. S23). On the basis of this particle size and of the average molecular dimensions determined with MD experiments, an average aggregation number between 280 and 350 molecules per aggregate can be estimated, in the case of a rodlike micelle.

Conclusions

In conclusion, in the present paper we have investigated the catalytic activity of the tetrafunctional calixarenes **3**-**5** in the cleavage of phosphodiesters. Their activity was explored over a wide concentration range and a sudden increase in reaction rates was observed in the correspondence of the CAC. An exhaustive kinetic investigation and elaboration of the experimental data was carried out in order to compare the activity of the catalysts free (as monomer, unaggregated) in solution with that in the aggregated systems. The picture obtained from this analysis points to an apparent superior cooperativity of the catalytic units upon aggregation and therefore to the existence of a remarkable dynamic preorganization in the assemblies. The evident advantage of the assemblies leads to believe monomer molecules in the aggregates can mold, flex and rearrange, to allow the catalytic units to reach an optimal fitting with the substrate.

Conflicts of interest

There are no conflicts to declare about the authors.

Acknowledgements

The authors thank the Tor Vergata University - Progetti Beyond Borders 2019 (E84I19002340005) and Progetti Ricerca Scientifica d'Ateneo 2021 (grant id: E83C22002730005). Moreover they thank the Italian Ministry of Instruction, University and Research programme (COMP- HUB initiative, Departments of Excellence Program and PRIN 2017E44A9P) for financial support.

Experimental Section

Instruments and General Methods. NMR spectra were recorded on a Bruker 700 MHz spectrometer. Chemical shifts are reported as δ values in ppm. Mass spectra analyses were

performed by an electrospray ionization time-of-flight spectrometer. The automatic titrator was equipped with a combined microglass pH electrode. All reactions, with the exception of the deprotection of **7** and **8**, were carried out under a nitrogen atmosphere. Flash chromatography was carried out on 70−230 mesh silica gel. Anhydrous DCM was obtained by distillation over calcium chloride and stored with molecular sieves.

Materials. Ultrapure mQ water was used for the preparation of solution. HPNP[56] and **3**-**5**[45-46] were prepared as reported in the literature. Other solvents and reagents were commercially available and used without any further purification. Warning! Tetramethylammonium perchlorate should been handled with care[57] as it is potentially explosive.

*4-(octyloxy)aniline (**6**).* To a solution of p-Nitrophenol (3g, 21.6mmol) in dry DMF (50 mL), NaH (60 wt.-% in oil 1.73 g, 43.2 mmol) was added at 0°C. The mixture was stirred for 30 min. then 1-bromooctane (8.34 g, 43.2 mmol) was added. After 1h the ice bath was removed and the reaction was heated to 80°C for 6h. The reaction was quenched with 1 M HCl (150 mL), the solvent was then removed under reduced pressure. The crude product was dissolved in 1 M HCl (30 mL) then washed with CH_2Cl_2 (30x3 mL). The organic phase was separated, dried over anhydrous Na_2SO_4 and evaporated under reduced pressure to obtain a brownish oil. The residue was purified by column chromatography on silica gel (hexane-hexane/AcOEt 60:1) to obtain the alkylated nitrophenol as a yellow oil in 30% yield (1.64 g, 6.52 mmol). The p-Nitro-4-(octyloxy)benzene (1.4 g, 5.57 mmol) was then dissolved in EtOH (250 mL) and the reduction of the Nitro group was carried out with N_2H_5OH (2.8 g, 55.7 mmol) and catalytic amount of Pd/C. The reaction was heated at 80°C for 6 hours then stirred for 3 days. The solution was then filtered through celite, the solvent was removed under reduced pressure. The crude product was dissolved in CH_2Cl_2 (30 mL) then washed with Na_2CO_3 saturated solution (3x15 mL). Pure aniline **6** (0.96 g, 4.37 mmol) was obtained after evaporation under reduced pressure as brown crystals in 79% yield. ^{1}H NMR (700 MHz, $CDCl_3$): δ 6.75 (d, J= 8.80 Hz, 2H), δ 6.64 (d, J=8.21 Hz, 2H), δ 3.88 (t, J=3.5 Hz, 2H), δ 3.35 (bs, 2H), δ 1.74 (d J=6.7 Hz, 2H), δ 1.44 (m, 2H), δ 1.30 (m, 8H), δ 0.89 (t, J=6.8 Hz, 3H). ^{13}C NMR (175 MHz, $CDCl_3$): δ 152.4, 139.5, 116.5, 115.6, 68.7, 31.8, 29.4, 29.3, 29.2, 26.0, 22.6, 14.0. m/z calcd for $C_{14}H_{24}NO$ $[M + H]^+$ 222.1858; found 222.1834.

4-(octyloxy)phenyl-N,N'-bis(tert-butoxycarbonyl)guanidine (**7**). The compound **6** (0.15 g, 0.68 mmol) was dissolved in CH_2Cl_2 (30 mL). Then N,N′-bis-(t-butoxycarbonyl)-N″-triflyl-guanidine (0.20 g, 0.511 mmol) was added and the reaction was stirred for 4 days. The solvent was removed under reduced pressure. The crude product was dissolved in $NaHSO_4$ (15 mL), washed with $NaHCO_3$ (3x15 mL) then evaporated under reduced pressure. The residue was purified by column

chromatography on silica gel (hexane/AcOEt 20:1) to obtain the pure product **7** as a white solid (0.126 g, 0.27 mmol). Yield: 52%. ^{1}H NMR (700 MHz, $CDCl_3$): δ 11.65 (bs, 1 H), δ 10.17 (bs, 1H), δ 7.45 (d, J=8.9 Hz, 2H), δ 6.84 (d, 2H), δ 3.94 (t, J=6.57 Hz, 2H), δ 1.75 (m, 2H), δ 1.53 (s, 9H),, δ 1.48 (s, 9H) δ 1.43 (m, 2H), δ 1.36-1.24 (m, 8H), δ 0.88 (t, J=6.8 Hz, 3H). ^{13}C NMR (175 MHz, $CDCl_3$): δ 156.3, 153.5, 153.3 129.5, 125.8, 123.7, 114.6, 83.4, 79.3, 68.2, 31.7, 29.3, 29.16, 29.15, 28.1, 28.0, 25.9, 22.6, 14.0. m/z calcd for $C_{25}H_{42}N_3O_5$ [M + H]+ 464.3124; found 464.3107.

*1-(4-(octyloxy)phenyl)guanidine (**1**).* The compound **7** (20 mg, 0.043 mmol) was dissolved in TFA/H_2O mixture (95:5 5mL) for 15h. The solvent was removed under reduced pressure. The residue was dissolved in 100 mL of a solution of HCl in EtOH (1.0 M). The mixture was evaporated at reduced pressure and the product was obtained with no further purification as a pale-yellow oil (12 mg, 0.040 mmol). Yield: 93%. ^{1}H NMR (700 MHz, CD_3OD): δ 7.19 (d, J=8.8 Hz, 2H), δ 7.00 (d, J=8.8 Hz, 2H), δ 3.99 (t, J=6.4 Hz, 2H), δ 1.78 (m, 2H), δ 1.48 (m, 2H), δ 1.35 (m, 8H), δ 0.91 (t, J=6.97 Hz, 3H). ^{13}C NMR (175 MHz, CD_3OD): δ 160.3, 158.6, 128.8, 128.0, 116.7, 69.3, 33.0, 30.5, 30.4, 30.3, 27.1, 23.7, 14.4. m/z calcd for $C_{15}H_{27}N_3O$ [M + H]+ 265.2149; found 265.2168.

*[N_α-Boc-N_ω-Pbf]-(4-octyloxyphenyl)argininamide (**8**).* To a stirring solution of Boc-Arg-PbfOH (0.54 g, 1.02 mmol) in dry DMF (20 mL), HOBt (0.15 g, 1.10 mmol) and DCC (0.21 g, 1.02 mmol) were added. After 15 min, a solution of **6** (0.15 g, 1.02 mmol) in dry DMF (3 mL) was added dropwise to the mixture which it was stirred for 48h at room temperature. The solution was filtered with a filter paper to remove the DCU and the solvent was removed under reduced pressure. The crude product was dissolved in ethyl acetate (15 mL), washed with Na_2CO_3 saturated solution (3x10 mL) and evaporated under reduced pressure. The pure product **8** was isolated by column chromatography on silica gel (hexane/AcOEt 3:1-hexane/AcOEt 1:2) as white crystals (0.163 g, 0.22 mmol). Yield: 21%. ^{1}H NMR (700 MHz, CD_3OD): 7.42 (d, J=8.9 Hz, 2H), δ 6.80 (d, J=8.9, 2H), δ 4.18 (dd, J=6.2 Hz, J=6.6 Hz, 1H), δ 3.88 (t, 2H, J=6.2), δ 3.27-3.10 (bm, 2H), δ 2.91 (s, 2H), δ 2.56 (s, 3H), δ 2.08 (s, 3H), δ 2.49 (s, 3H), 1.82-1.53 (bm, 6H), δ 1.46-1.36 (bm, 17H), δ 0.88 (t, J=6.8 Hz, 3H). ^{13}C NMR (175 MHz, CD_3OD): δ 172.9, 160.0, 158.0, 157.7, 157.3, 139.3, 134.2, 133.4, 132.1, 125.9, 123.2, 118.3, 115.5, 87.5, 80.6, 69.1, 56.1, 43.9, 41.4, 32.9, 30.9, 30.4, 30.4, 30.3, 28.8, 27.1, 23.6, 19.7, 18.45, 14.5, 12.6, 9.6. m/z calcd for $C_{38}H_{60}N_5O_7S$ $[M + H]^+$ 730.4213; found 730.4192; m/z calcd for $C_{38}H_{59}N_5O_7SNa$ $[M + Na]^+$ 752.4033, found 752.4014.

(4-octyloxyphenyl)argininamide (**2**). Compound **8** (80 mg, 0.11 mmol) was dissolved in TFA/MeOH/TIS (90/8/2, 5 mL) for 48h. The solvent was then removed under reduced pressure and washed in diethyl ether (3x5 mL). The residue was dissolved with 50 mL of a solution of HCl in EtOH. The crude product was then dried under reduced pressure to obtain the product **2** as a sticky colourless oil. (7.2 mg, 16 μmol). Yield: 15%. ^{1}H NMR (700 MHz, CD_3OD): δ 7.50 (d, J=8.6 Hz,

2H), δ 6.88 (d, J=8.6 Hz, 2H), δ 4.04 (t, J=6.4, 1H), δ 3.94 (t, J=6.4 Hz, 2H), δ 3.69 (s, 1H), δ 3.25 (t, J=6.6 Hz, 2H), δ 2.08-1.96 (bm, 2H), 1.75 (bm, 4H), δ 1.47 (bm, 2H), δ 1.40-1.28 (bm, 8H), δ 0.91 (t, 3H, J=6.8 Hz, 3H). ^{13}C NMR (175 MHz, CD_3OD): δ 168.1, 158.79, 158.78, 131.9, 123.1, 115.7, 69.3, 54.4, 41.5, 32.9, 30.4, 29.6, 27.1 24.8, 23.6, 14.3 m/z calcd for $C_{25}H_{44}N_5O_4$ $[M + H]^+$ 478.3388, found 478.3406.

Kinetic Measurements. Cleavage of HPNP and BNPP was monitored spectrophotometrically following the liberation of *p*-nitrophenol at 400 nm. Initial rate measurements reported in Tables 1 and 2 were carried out in water solutions thermostated at 25 °C or 50 °C for HPNP or BNPP cleavage, respectively. The concentrations of the species in solutions are reported in the footnotes of the tables. The solutions were buffered with CHES and the pH was adjusted with 50-100 mM water solutions of $HClO_4$ or NaOH. The ionic strenght was buffered with Me_4NClO_4. The elaboration of the experimental data and the nonlinear least-square fitting procedures described in the text were carried out with the software SigmaPlot 12.0 (Systat Software, Inc.). The raw kinetic data are reported in the Supporting Informations.

Molecular Dynamics The MD simulations were performed using either the Gromacs 2019 software package with the modified Gromos54a7 force field,[58] or HyperChem 8.0.6 software. The SPC water model in a cubic box was used to solvate the investigated compound. Gromacs topologies of the investigated molecules were generated with Automated Topology Builder version 3.0. The other configurations of the Molecular Dynamic simulation were set up us previously reported.[14] The determination of the distances between the active units described in the main text was performed with the command mindist.

References

1. Kuah, E.; Toh, S.; Yee, J.; Ma, Q.; Gao, Z.; Enzyme Mimics: Advances and Applications. *Chem. Eur. J.* **2016,** *22*, 8404-30.
2. von Krbek, L. K. S.; Schalley, C. A.; Thordarson, P.; Assessing cooperativity in supramolecular systems. *Chem. Soc. Rev.* **2017,** *46*, 2622-2637.
3. Badjica, J. D.; Nelson, A.; Cantrill, S. J.; Turnbull, W. B.; Stoddart, J. F.; Multivalency and Cooperativity in Supramolecular Chemistry. *Acc. Chem. Res.* **2005,** *38*, 723-732.
4. Ercolani, G.; Assessment of Cooperativity in Self-Assembly. *J. Am. Chem. Soc.* **2003,** *125*, 16097-16103.
5. Marchetti, L.; Levine, M.; Biomimetic Catalysis. *ACS Catalysis* **2011,** *1*, 1090-1118.
6. Dong, Z.; Luo, Q.; Liu, J.; Artificial enzymes based on supramolecular scaffolds. *Chem. Soc. Rev.* **2012,** *41*, 7890-7908.
7. Raynal, M.; Ballester, P.; Vidal-Ferran, A.; van Leeuwen, P. W.; Supramolecular catalysis. Part 2: artificial enzyme mimics. *Chem. Soc. Rev.* **2014,** *43*, 1734-87.

8. Kofoed, J.; Reymond, J.; Dendrimers as artificial enzymes. *Curr. Opin. Chem. Biol.* **2005,** *9*, 656-664.
9. Wulff, G.; Liu, J.; Design of Biomimetic Catalysts by Molecular Imprinting in Synthetic Polymers: The Role of Transition State Stabilization. *Acc. Chem. Res.* **2012,** *45*, 239-247.
10. Nothling, M. D.; Xiao, Z.; Bhaskaran, A.; Blyth, M. T.; Bennett, C. W.; Coote, M. L.; Connal, L. A.; Synthetic Catalysts Inspired by Hydrolytic Enzymes. *ACS Catalysis* **2018,** *9*, 168-187.
11. Wu, J.; Wang, X.; Wang, Q.; Lou, Z.; Li, S.; Zhu, Y.; Qin, L.; Wei, H.; Nanomaterials with enzyme-like characteristics (nanozymes): next-generation artificial enzymes (II). *Chem. Soc. Rev.* **2019,** *48*, 1004-1076.
12. Salvio, R.; The Guanidinium Unit in the Catalysis of Phosphoryl Transfer Reactions: From Molecular Spacers to Nanostructured Supports. *Chem. Eur. J.* **2015,** *21*, 10960-71.
13. Lyu, Y.; Scrimin, P.; Mimicking Enzymes: The Quest for Powerful Catalysts from Simple Molecules to Nanozymes. *ACS Catalysis* **2021**, 11501-11509.
14. Salvio, R.; D'Abramo, M.; Conformational Mobility and Efficiency in Supramolecular Catalysis. A Computational Approach to Evaluate the Performances of Enzyme Mimics. *Eur. J. Org. Chem.* **2020**, 6004-6011.
15. Joshi, T.; Graham, B.; Spiccia, L.; Macrocyclic metal complexes for metalloenzyme mimicry and sensor development. *Acc. Chem. Res.* **2015,** *48*, 2366-79.
16. Cacciapaglia, R.; Di Stefano, S.; Mandolini, L.; Salvio, R.; Reactivity of carbonyl and phosphoryl groups at calixarenes. *Supramol. Chem.* **2013,** *25*, 537-554.
17. Schroeder, G. K.; Lad, C.; Wyman, P.; Williams, N. H.; Wolfenden, R.; The time required for water attack at the phosphorus atom of simple phosphodiesters and of DNA. *PNAS* **2006,** *103*, 4052-5.
18. Wolfenden, R.; Degrees of Difficulty of Water-Consuming Reactions in the Absence of Enzymes. *Chem. Rev.* **2006,** *106*, 3379-3396.
19. Mancin, F.; Scrimin, P.; Tecilla, P.; Progress in artificial metallonucleases. *Chem. Commun.* **2012,** *48*, 5545-59.
20. Lönnberg, H.; Cleavage of RNA phosphodiester bonds by small molecular entities: a mechanistic insight. *Org. Biomol. Chem.* **2011,** *9*, 1687-1703.
21. Diez-Castellnou, M.; Mancin, F.; Scrimin, P.; Efficient phosphodiester cleaving nanozymes resulting from multivalency and local medium polarity control. *J. Am. Chem. Soc.* **2014,** *136*, 1158-61.
22. Salvio, R.; Cacciapaglia, R.; Mandolini, L.; Sansone, F.; Casnati, A.; Diguanidinocalix[4]arenes as effective and selective catalysts of the cleavage of diribonucleoside monophosphates. *RSC Adv.* **2014,** *4*, 34412-34416.
23. Salvio, R.; Moliterno, M.; Caramelli, D.; Pisciottani, L.; Antenucci, A.; D'Amico, M.; Bella, M.; Kinetic resolution of phosphoric diester by Cinchona alkaloid derivatives provided with a guanidinium unit. *Catal. Sci. Technol.* **2016,** *6*, 2280–2288.
24. Salvio, R.; Volpi, S.; Folcarelli, T.; Casnati, A.; Cacciapaglia, R.; A calix[4]arene with acylguanidine units as an efficient catalyst for phosphodiester bond cleavage in RNA and DNA model compounds. *Org. Biomol. Chem.* **2019,** *17*, 7482-7492.
25. Salvio, R.; Volpi, S.; Cacciapaglia, R.; Sansone, F.; Mandolini, L.; Casnati, A.; Phosphoryl Transfer Processes Promoted by a Trifunctional Calix[4]arene Inspired by DNA Topoisomerase I. *J. Org. Chem.* **2016,** *81*, 9012−9019.
26. Ren, C. Z. J.; Solís-Muñana, P.; Warr, G. G.; Chen, J. L. Y.; Dynamic and Modular Formation of a Synergistic Transphosphorylation Catalyst. *ACS Catalysis* **2020,** *10*, 8395-8401.
27. Wirth-Hamdoune, D.; Ullrich, S.; Scheffer, U.; Radanovic, T.; Durner, G.; Gobel, M. W.; A Bis(guanidinium)alcohol Attached to a Hairpin Polyamide: Synthesis, DNA Binding, and Plasmid Cleavage. *ChemBioChem* **2016,** *17*, 506-14.
28. Laine, M.; Lönnberg, T.; Helkearo, M.; Lönnberg, H.; Cleavage of short oligoribonucleotides by a Zn2+ binding multi-nucleating azacrown conjugate. *Inorg. Chim. Acta* **2016,** *452*, 111-117.

29. Wang, Y.; Liu, E.; Lam, C. H.; Perrin, D. M.; A densely modified M2+-independent DNAzyme that cleaves RNA efficiently with multiple catalytic turnover. *Chem. Sci.* **2018,** *9*, 1813-1821.
30. Mohamed, M. F.; Brown, R. S.; Cleavage of an RNA Model Catalyzed by Dinuclear Zn(II) Complexes Containing Rate-Accelerating Pendants. Comparison of the Catalytic Benefits of H-Bonding and Hydrophobic Substituents. *J. Org. Chem.* **2010,** *75*, 8471-8477.
31. Salvadeo, E.; Dubois, L.; Latour, J.-M.; Trinuclear copper complexes as biological mimics: Ligand designs and reactivities. *Coord. Chem. Rev.* **2018,** *374*, 345-375.
32. Daver, H.; Das, B.; Nordlander, E.; Himo, F.; Theoretical Study of Phosphodiester Hydrolysis and Transesterification Catalyzed by an Unsymmetric Biomimetic Dizinc Complex. *Inorg. Chem.* **2016,** *55*, 1872-1882.
33. Ruiz Kubli, M.; Yatsimirsky, A. K.; Phosphodiester cleavage by trivalent lanthanides in the presence of native cyclodextrins. *Inorg. Chim. Acta* **2016,** *440*, 9-15.
34. Subat, M.; Woinaroschy, K.; Gerstl, C.; Sarkar, B.; Kaim, W.; Konig, B.; 1,4,7,10-tetraazacyclododecane metal complexes as potent promoters of phosphodiester hydrolysis under physiological conditions. *Inorg. Chem.* **2008,** *47*, 4661-8.
35. Bim, D.; Svobodova, E.; Eigner, V.; Rulisek, L.; Hodacova, J.; Copper(II) and Zinc(II) Complexes of Conformationally Constrained Polyazamacrocycles as Efficient Catalysts for RNA Model Substrate Cleavage in Aqueous Solution at Physiological pH. *Chem. Eur. J.* **2016,** *22*, 10426-37.
36. Gruber, B.; Kataev, E.; Aschenbrenner, J.; Stadlbauer, S.; Konig, B.; Vesicles and micelles from amphiphilic zinc(II)-cyclen complexes as highly potent promoters of hydrolytic DNA cleavage. *J. Am. Chem. Soc.* **2011,** *133*, 20704-7.
37. Poznik, M.; Maitra, U.; Konig, B.; The interface makes a difference: lanthanide ion coated vesicles hydrolyze phosphodiesters. *Org. Biomol. Chem.* **2015,** *13*, 9789-92.
38. Salvio, R.; Casnati, A.; Guanidinium Promoted Cleavage of Phosphoric Diesters: Kinetic Investigations and Calculations Provide Indications on the Operating Mechanism. *J. Org. Chem.* **2017,** *82*, 10461-10469.
39. Salvio, R.; Casnati, A.; Mandolini, L.; Sansone, F.; Ungaro, R.; ATP cleavage by cone tetraguanidinocalix[4]arene. *Org. Biomol. Chem.* **2012,** *10*, 8941 - 8943.
40. Salvio, R.; Volpi, S.; Cacciapaglia, R.; Sansone, F.; Mandolini, L.; Casnati, A.; Upper Rim Bifunctional cone-Calix[4]arenes Based on a Ligated Metal Ion and a Guanidinium Unit as DNAase and RNAase Mimics. *J. Org. Chem.* **2016,** *81*, 4728-35.
41. Savelli, C.; Salvio, R.; Guanidine-Based Polymer Brushes Grafted onto Silica Nanoparticles as Efficient Artificial Phosphodiesterases. *Chem. Eur. J.* **2015,** *21*, 5856-5863.
42. Rebilly, J.-N.; Reinaud, O.; Calixarenes and resorcinarenes as scaffolds for supramolecular metallo-enzyme mimicry. *Supramol. Chem.* **2014,** *26*, 454-479.
43. Montalbetti, C. A. G. N.; Falque, V.; Amide bond formation and peptide coupling. *Tetrahedron* **2005,** *61*, 10827-10852.
44. Konig, W.; Geiger, R.; A new method for synthesis of peptides: activation of the carboxyl group with dicyclohexylcarbodiimide using 1-hydroxybenzotriazoles as additives. *Chem. Ber.* **1970,** *103*, 788-798.
45. Bagnacani, V.; Franceschi, V.; Bassi, M.; Lomazzi, M.; Donofrio, G.; Sansone, F.; Casnati, A.; Ungaro, R.; Arginine clustering on calix[4]arene macrocycles for improved cell penetration and DNA delivery. *Nat. Commun.* **2013,** *4*, 1721.
46. Sansone, F.; Dudic, M.; Donofrio, G.; Rivetti, C.; Baldini, L.; Casnati, A.; Cellai, S.; Ungaro, R.; DNA Condensation and Cell Transfection Properties of Guanidinium Calixarenes: Dependence on Macrocycle Lipophilicity, Size, and Conformation. *J. Am. Chem. Soc.* **2006,** *128*, 14528-14536.
47. Salvio, R.; Mandolini, L.; Savelli, C.; Guanidine-Guanidinium Cooperation in Bifunctional Artificial Phosphodiesterases Based on Diphenylmethane Spacers; gem-Dialkyl Effect on Catalytic Efficiency. *J. Org. Chem.* **2013,** *78*, 7259-63.

48. Pineiro, L.; Novo, M.; Al-Soufi, W.; Fluorescence emission of pyrene in surfactant solutions. *Adv. Colloid Interface Sci.* **2015,** *215*, 1-12.
49. Bains, G.; Patel, A. B.; Narayanaswami, V.; Pyrene: a probe to study protein conformation and conformational changes. *Molecules* **2011,** *16*, 7909-35.
50. Kalyanasundaram, K.; Thomas, J. K.; Environmental Effects on Vibronic Band Intensities in Pyrene Monomer Fluorescence and Their Application in Studies of Micellar Systems. *J. Am. Chem. Soc.* **1977,** *99*, 2039-2044.
51. Lindman, B.; Holmberg, K.; Shah, D. O.; Schwuger, M. O.; Eds., *Handbook of Applied Surface and Colloid Chemistry, 1*. John Wiley & Sons, New York, NY (2002)
52. Nagarajan, R.; Molecular Packing Parameter and Surfactant Self-Assembly: The Neglected Role of the Surfactant Tail. *Langmuir* **2002,** *18*, 31-38.
53. Khalil, R. A.; Zarari, A.-h. A.; Theoretical estimation of the critical packing parameter of amphiphilic self-assembled aggregates. *Appl. Surf. Sci.* **2014,** *318*, 85-89.
54. Kobierski, J.; Wnetrzak, A.; Chachaj-Brekiesz, A.; Dynarowicz-Latka, P.; Predicting the packing parameter for lipids in monolayers with the use of molecular dynamics. *Colloids Surf. B: Biointerfaces* **2022,** *211*, 112298.
55. Stetefeld, J.; McKenna, S. A.; Patel, T. R.; Dynamic light scattering: a practical guide and applications in biomedical sciences. *Biophys. Rev.* **2016,** *8*, 409-427.
56. Brown, D. M.; Usher, D. A.; *J. Chem. Soc.* **1965**, 6558–6564.
57. Luxon, S. G., Ed., *Hazards in the Chemical Laboratory, 5th ed.* The Royal Society of Chemistry: Cambridge, UK, 1992; p 524.
58. Schmid, N.; Eichenberger, A. P.; Choutko, A.; Riniker, S.; Winger, M.; Mark, A. E.; van Gunsteren, W. F.; Definition and testing of the GROMOS force-field versions 54A7 and 54B7. *Eur. Biophys. J.* **2011,** *40*, 843-56.